THE JOURNAL OF PHYSICAL CHEMISTRY Letters

Letter

Cite This: J. Phys. Chem. Lett. 2017, 8, 5501-5506

pubs.acs.org/JPCL

Fingerprints of Both Watson−Crick and Hoogsteen Isomers of the Isolated (Cytosine-Guanine)H$^+$ Pair

Andrés F. Cruz-Ortiz,[†,‡] Maximiliano Rossa,[†,‡] Francis Berthias,[§] Matías Berdakin,[†,‡,⊥] Philippe Maitre,*[,§] and Gustavo A. Pino*[,†,‡]

[†]Instituto de Investigaciones en Fisicoquímica de Córdoba (INFIQC), CONICET − UNC, Ciudad Universitaria, X5000HUA Córdoba, Argentina

[‡]Dpto. de Fisicoquímica, Facultad de Ciencias Químicas, Centro Láser de Ciencias Moleculares, Universidad Nacional de Córdoba, Ciudad Universitaria, X5000HUA Córdoba, Argentina

[§]Laboratoire de Chimie Physique, Université Paris-Sud, CNRS, Université Paris-Saclay, F-91405 Orsay, France

Supporting Information

ABSTRACT: Gas phase protonated guanine-cytosine (CGH$^+$) pair was generated using an electrospray ionization source from solutions at two different pH (5.8 and 3.2). Consistent evidence from MS/MS fragmentation patterns and differential ion mobility spectra (DIMS) point toward the presence of two isomers of the CGH$^+$ pair, whose relative populations depend strongly on the pH of the solution. Gas phase infrared multiphoton dissociation (IRMPD) spectroscopy in the 900−1900 cm^{-1} spectral range further confirms that the Watson−Crick isomer is preferentially produced (91%) at pH = 5.8, while the Hoogsteen isomer predominates (66%) at pH = 3.2. These fingerprint signatures are expected to be useful for the development of new analytical methodologies and to trigger isomer selective photochemical studies of protonated DNA base pairs.

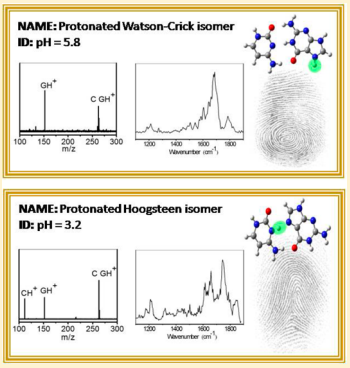

One decade after Watson and Crick (WC) discovered the double-helix structure of DNA,[1] Hoogsteen (Hoo)[2] reported a crystal structure in which the base pair had a different geometry from that reported by WC. The same year, 1963, Löwdin proposed that a proton transfer (PT) reaction within the WC pair could give rise to point mutations by formation of rare tautomers.[3] The activation energy barriers for the PT reaction between the bases are on the order of 58−67 kJ/mol,[4] and then at room temperature, this process can only take place by tunneling. However, it has been suggested that these barriers are strongly reduced upon ionization[4−6] or protonation of the base pair.[4]

Protonation of the nucleobases is also known to induce the formation of proton-mediated Hoo pairs.[7] These protonated species play an important role in many biological processes because they can alter DNA structure by the formation of triple helices, affecting its biological reactivity.[8] WC isomers are more stable than Hoo structures under physiological pH. However, it has been shown that under specific conditions their stabilities can be comparable or even inverted.[9−11]

Hoo-mediated triplexes have been shown to be involved in the development of diseases as in the case of the Friedreich's ataxia[12] and other human diseases recently reviewed.[13] It has been also proved that formation of a triplex can induce mutations at specific genomic sites in somatic cells of adult mice.[14]

More recently, transient Hoo pairs inside of canonical duplex DNA and specifically bound to transcription factors and damaged sites were observed.[11,15,16] This observation opened a new paradigm, suggesting that the DNA double helix may also code for transient Hoo pairs as a way of expanding the genetic code beyond that achieved based on WC base pairing.[15,16]

In this context, it thus seems that detailed studies at the molecular level of a protonated DNA base pairing process is of high importance for a better understanding of biological chemistry of DNA. However, rare tautomers and specific protonation sites within the pairs are hardly detectable by the biological machinery, and very complicated and time-consuming experiments such as X-ray crystal diffraction[17] or NMR nuclear relaxation experiments[15] have been used to structurally characterize these species. In addition, many theoretical efforts have been done to understand these phenomena,[4,7,8,18,19] which need benchmark gas-phase experimental data to prove their validity and universality.

The latest advances in tandem mass spectrometry (MS/MS) for biological systems[20] and its recent coupling to UV and/or IR vibrational spectroscopy have allowed studying small proton/metal-bonded complexes,[6,21−26] and in this sense, the five protonated bases[27−30] and the protonated pyridine

Received: August 14, 2017
Accepted: October 24, 2017
Published: October 24, 2017

DOI: 10.1021/acs.jpclett.7b02140
J. Phys. Chem. Lett. 2017, 8, 5501−5506

homodimers[31,32] were characterized so far. On the other hand, the coupling of ion mobility to MS/MS, which relies on the interactions of ions with a buffer gas at nearly atmospheric pressure,[33] allows for the separation of isomeric species, which can then be probed by MS/MS.[34]

The goal of this work is to report a method to probe the effect of protonation on the pairing pattern of a cytosine-guanine (CGH^+) pair in solution, either in the WC or Hoo isomeric structures using tandem mass spectrometry. CGH^+ ions generated by electrospray ionization (ESI) are characterized by MS/MS, infrared multiphoton dissociation (IRMPD) spectroscopy, and differential ion mobility spectrometry (DIMS), and it is shown that fingerprints of each pattern can be derived. This is a very fast method to classify WC and Hoo pairs and determine the protonation site of the dimer.

Two solutions containing equal concentrations of C and G were prepared in methanol/water 50:50 solvent, as explained in the Experimental and Computational Methods section. The pH of solution A was 5.8, while in the case of solution B the acidity was increased up to pH = 3.2. In both cases, the CGH^+ ion (m/z 263) was mass-selected and subsequently fragmented in a hybrid FT-ICR mass spectrometer by collision induced dissociation (CID) or IRMPD by irradiation with a free-electron laser (FEL) of CLIO,[35] assisted or not by a CO_2 laser.[36] Using IR-FEL, infrared multiple photon absorption provides a slow heating process of molecular ions. As shown below, the fragmentation patterns are very similar to those observed when ions are subjected to multiple low-energy collisions with rare gas atoms. The total intensity of parent ions in solution B was 1.5 times higher than that in solution A.

Figure 1 shows that the fragmentation pattern upon IRMPD strongly depended on the solution used to prepare the parent

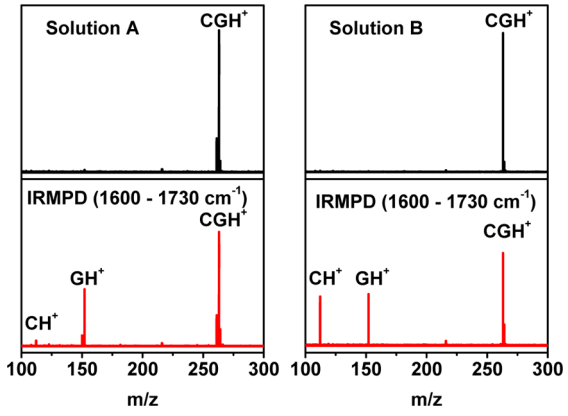

Figure 1. MS/MS of an isolated CGH^+ protonated pair before fragmentation (upper panels) produced from solution A (left) and solution B (right) and after fragmentation by IRMPD for which the fragmentation MS was summed over the spectral range of 1600−1730 cm^{-1} (lower panels).

ion. For solution A, the fragment m/z 152 corresponding to GH^+ was mainly observed with a small contribution of the fragment m/z 112 corresponding to CH^+ (<10%), while in the case of solution B, both fragments m/z 152 (GH^+) and m/z 112 (CH^+) were detected at similar intensities, CH^+ (49%) and GH^+ (51%) (Figure 1). The different fragmentation patterns suggest that different structures are populated in each solution.

In order to challenge this hypothesis, DIMS experiments have been carried out in order to separate CGH^+ isomers (m/z 263) and eventually characterize the isomer specific fragmentation patterns through subsequent MS/MS.

The DIMS spectra recorded for solutions A and B are reported in Figure 2. In panel a, the abundance of m/z 263 is

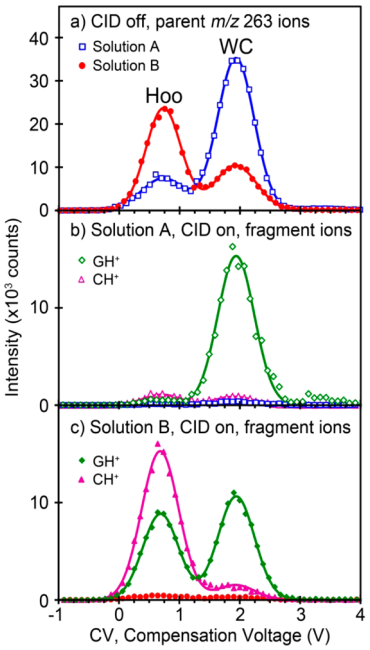

Figure 2. (a) DIMS spectra of the parent ion CGH^+ (m/z 263) generated from solution A (blue open squares) and solution B (red filled circles). (b,c) DIMS-MS/MS(CID) spectra generated from CID (collision voltage 0.2 V with He) of the parent ion CGH^+ (m/z 263) produced from solution A and solution B, respectively. In these two panels, in addition to the CGH^+ parent ions, ion counts for the daughter ions GH^+ (m/z 152, green diamond) and CH^+ (m/z 112, pink triangle) are also given. The solid lines are the result of the fits to two Gaussian distributions in each spectrum. Dinitrogen is used for the desolvation and DIMS carrier gas. The dispersion voltage is set to 1800 V.

plotted against the compensation voltage (CV) and the experimental data are fitted to Gaussian functions. For both solutions, two peaks centered at CV (0.76 ± 0.07) and (1.92 ± 0.07) V were observed, suggesting the presence of the same two isomers of the m/z 263 ion but at significantly different relative populations at the two pH values of the solution. For solution A, the relative populations of the isomers appearing at CV 0.76 and 1.92 V were (10 ± 5) and (90 ± 5)%, respectively, while in solution B, these populations were (70 ± 5) and (30 ± 5)%, respectively.

Figure 2b,c shows DIMS-MS/MS(CID) spectra. For each peak, DIMS and mass-selected m/z 263 ions were subjected to CID. For both solutions, and a CV value set at 1.92 V, the two GH^+ and CH^+ fragments are observed, with relative contributions of (91 ± 3) and (9 ± 3)%, respectively. At a CV value of 0.76 V, however, the two GH^+ and CH^+ fragments are also observed but with relative contributions of (34 ± 2) and (66 ± 2)%, respectively, for the two solutions. The reported yields are the averages of both solutions at each CV.

The DIMS spectra shown in Figure 2a thus provide evidence for the formation of the same two isomers, hereafter called $CGH^+(0.76)$ and $CGH^+(1.92)$, produced in significantly different proportions at each pH value. In addition, the DIMS-MS/MS(CID) spectra in panels b and c of Figure 2

DOI: 10.1021/acs.jpclett.7b02140
J. Phys. Chem. Lett. 2017, 8, 5501−5506

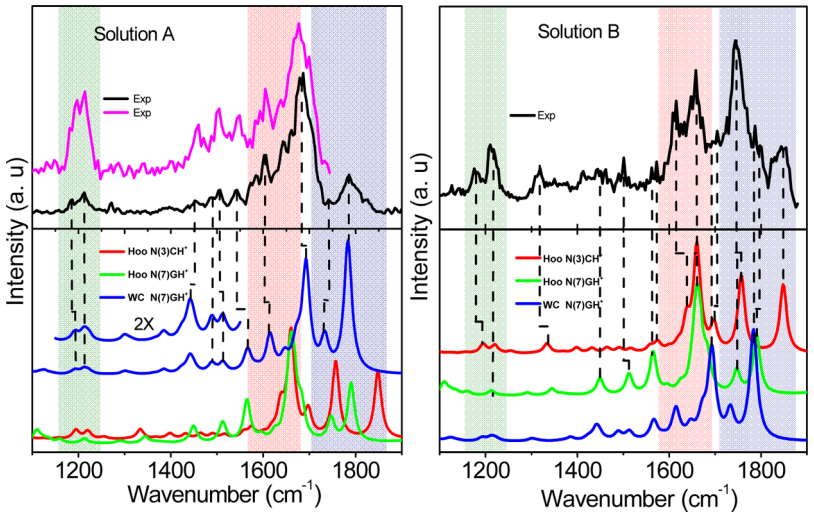

Figure 3. IRMPD spectra of the parent ion CGH^+ (m/z 263) (upper panels) produced from solution A (left) and solution B (right) upon 250 ms of FEL irradiation time. The pink line (upper-left panel) was recorded with a FEL irradiation time of 500 ms. The lower panels show the calculated linear absorption IR spectra (M06-2X/6-311G++(d,p)) that best fit the experimental one: the most stable WC isomer protonated on $N(7)GH^+$ (blue) and the Hoo isomers with the proton closer to $N(3)CH^+$ (red) or to $N(7)GH^+$ (green). The vibrational frequencies were corrected by a factor of 0.983.[38] The three spectral regions highlighted in color bars are discussed below.

provide evidence for the different fragmentation patterns of these two isomers. The $CGH^+(1.92)$ isomer is the most abundant isomer in solution A (90%), which is selectively (91%) fragmented into GH^+. The $CGH^+(0.76)$ isomer is the dominant isomer (70%) in more acid conditions, as in solution B, which is fragmented into both GH^+ (34%) and CH^+ (66%).

The total contributions of GH^+ and CH^+ to the MS/MS spectra of the parent ion obtained from solutions A and B without DIMS selection is given by the partial contribution of both isomers to each fragment. Considering solution A, the total contributions of GH^+ and CH^+ are (85 ± 9) and (15 ± 7)%, respectively. In the same manner, the total contributions of GH^+ and CH^+ in solution B are (51 ± 8) and (49 ± 5)%, respectively. These results are in very good agreement with those obtained by MS/MS-IRMPD (Figure 1).

In order to assign the structures of the two $CGH^+(0.76)$ and $CGH^+(1.92)$ isomers preferentially populated at the different pHs, the IRMPD spectra of the parent ion CGH^+ (m/z 263) were recorded.

The IRMPD spectra of the CGH^+ ions produced from solutions A and B are shown in Figure 3, together with the simulated linear IR absorption spectra of the relevant isomers for this work. A broad variety of CGH^+ structures, generated from the most abundant neutral and protonated tautomers of C and G in solution (see the SI), were optimized with the hybrid density functional theory at the M06-2X/6-311G++(d,p) level. The solvent effect on the electronic energy was accounted for in the Dielectric Polarizable Continuum Model (D-PCM). All of the calculations were performed with the Gaussian 09 suite of programs.[37] All of the calculated structures and their relative energies and standard Gibbs free energy at 298 K ($\Delta G_{298\ K}$), including the zero-point energy (ZPE) correction, are reported in the SI (Table SI1).

Figure 4 shows the relevant isomers for the discussion of this work. Among the different isomers, the two Hoo pairs are the most stable structures of the CGH^+ protonated dimer in the gas phase, while the protonated WC-$N(7)GH^+$ isomer lies at higher energy, as shown in Figure 4. However, as reported in

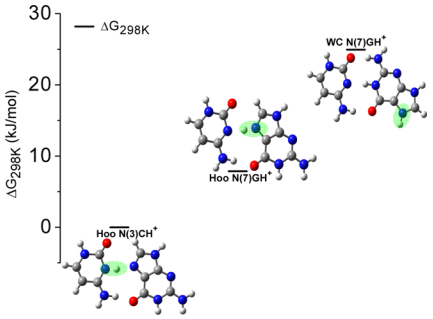

Figure 4. Most stable Hoo and WC structures of the protonated CGH^+ dimer, calculated at the M06-2X/6-311G++(d,p) level with the Gaussian 09 suite of programs.[37] In the figure, the ΔG at 298 K is depicted. The green marks indicate the position of the H^+ in the dimer.

the literature,[9−11] the relative population of these isomers in solution strongly depends on the pH.[9−11]

The calculated IR spectra for these isomers are in good agreement with previous theoretical reports by other groups[7,19] and are shown in Figure 3 together with the experimental IRMPD spectra. A comparison with the calculated IR spectra of other low-energy isomers is reported in Figure SI1. Three regions of the IR spectra, highlighted in colors in Figure 3, are of special interest for the discussion.

The most structurally diagnostic region is the C═O stretching modes region (1700−1900 cm^{-1}). The IR spectrum associated with solution A has a fingerprint band at 1786 cm^{-1} that is assigned to the C═O stretching mode of G in the WC-$N(7)GH^+$ isomer (calculated at 1784 cm^{-1}). In the case of solution B, the band centered at 1848 cm^{-1} is assigned to the C═O stretching mode of C in the Hoo-$N(3)CH^+$ isomer (calculated at 1850 cm^{-1}), which is the only isomer with a predicted IR absorption band above 1800 cm^{-1}. The strong band at 1743 cm^{-1} in the case of solution B could also be assigned to an IR absorption band of the Hoo-$N(3)CH^+$ isomer calculated at 1749 cm^{-1}, corresponding to the C═O stretching mode of G. It should be noted, however, that the

DOI: 10.1021/acs.jpclett.7b02140
J. Phys. Chem. Lett. 2017, 8, 5501−5506

contribution of other isomers to the IRMPD spectrum of solution B cannot be excluded. For example, the Hoo-N(7)GH$^+$ isomer has a band predicted at 1748 cm^{-1} (C═O stretching mode of C) that could also contribute to the strong IRMPD band at 1743 cm^{-1}. Furthermore, this band is asymmetric, and its shoulder at 1797−1788 cm^{-1} could be assigned to the C═O stretching mode of G in the Hoo-N(7)GH$^+$ isomer (1790 cm^{-1}) and/or to the C═O stretching mode of G (1786 cm^{-1}) in the WC-N(7)GH$^+$ isomer.

The spectral assignments in the NH_2 bending and ring C−N stretching modes region (1600−1700 cm^{-1}) are consistent with those in the C═O stretching region. In the case of solution A, the intense band observed at 1687 cm^{-1} nicely matches the band of the WC-N(7)GH$^+$ isomer predicted at 1692 cm^{-1}. In solution B, a double peak at 1658 and 1615 cm^{-1} is observed in this region. The red shift of these features with respect to solution A is consistent with the predicted IR absorption spectra, and these two features could be assigned to the presence of both Hoo-N(3)CH$^+$ (1654 cm^{-1}) and Hoo-N(7)GH$^+$ (1662 cm^{-1}) isomers. Nonetheless, contribution from WC isomers, such as the WC-N(7)GH$^+$ isomer, cannot be excluded.

Finally, the IRMPD spectrum of solution B shows a double peak in the low-energy region. The peak at 1182 cm^{-1} correlates with the calculated peak at 1190 cm^{-1} for the Hoo-N(3)CH$^+$ isomer, while the most intense peak at 1217 cm^{-1} is assumed to be due to the peak calculated at 1215 cm^{-1} for the Hoo-N(3)CH$^+$ isomer and the one calculated at 1214 cm^{-1} for the Hoo-N(7)GH$^+$, resulting in a higher intensity.

IRMPD spectroscopy in the 1100−1900 cm^{-1} range thus allows for structural assignment of the two isomers identified by DIMS. A WC structure, more precisely the WC-N(7)GH$^+$ protomer, can be assigned to isomer CGH$^+$(1.92), which is found to be preferentially formed from solution A. In the case of the CGH$^+$(0.76) isomer, which is found to be preferentially formed from solution B, the above analysis suggests that two Hoo structures should be considered, with the proton bounded to N(3)C or N(7)G. These two isomers exist in a double-well potential coupled by the proton motion whose frequency is 2526 and 2008 cm^{-1} for the N(3)C and N(7)G isomers, respectively, and connected through a low-energy barrier (12.4 kJ/mol, calculated at the M06-2X/6-311G++(d,p) level). Accounting for the ZPE of the proton motion between C and G, the ground-state vibrational level is located at 2.8 kJ/mol above the energy barrier (see Figure SI2). Therefore, both Hoo isomers should coexist in their ground state, independent of the temperature of the system.

As a conclusion, IRMPD and DIMS results provide evidence for a change of isomer population when the pH changes. At pH 5.8 (solution A), the most abundant isomer is a WC isomer, while at lower pH (3.2, solution B), Hoo isomers are the most abundant.

The WC pair is stable in solution A (pH = 5.8) and the most abundant CGH$^+$ isomer because Hoo pairs are not expected to efficiently compete with WC pairs, unless N(3)C (pK_a = 4.5)[39] or N(7)G (pK_a = 3.3)[39] is protonated,[10,11] although transient Hoo pairs with lifetimes of only 0.3−1.1 ms have been recently observed at higher pH.[11,15,16] The WC structure is retained upon the ESI process, where it is probably protonated on the available position of the dimer with the highest proton affinity (N(7)G) (see Table S1). Then, upon fragmentation by CID or IRMPD, the most abundant observed fragment is GH$^+$ (91 ± 3)% because fragmentation to CH$^+$ requires previous isomerization to one of the Hoo isomers. This isomerization involves a very large nuclear rearrangement, including the dissociation of two H-bonds of the WC isomer and the rotation of the GH$^+$ moiety, which is entropically disfavored. Experiments were carried out using irradiation with the FEL at full power and simultaneous CO_2 laser irradiation, but no change in the fragmentation pattern was observed. It thus seems that the isomerization rate is slower than the rate of direct dissociation to GH$^+$, which is a simple bond breaking, and as a consequence, the fragment CH$^+$ is hardly observed (9 ± 3)%.

In solution B (pH = 3.2), the concentration of protons allows the protonation of N(3)C (pK_a = 4.5) and N(7)G (pK_a = 3.3), and then, an appreciable concentration of the Hoo isomer can be produced and it becomes the most populated structure in solution, as expected from previous reports.[10,11] The Hoo structure is kept upon the ESI process, and it is likely that two Hoo isomers are formed because vibrational signatures from both are observed in the IRMPD spectrum. In addition, the ground-state vibrational level along the PT coordinate is located above the energy barrier for this process, ensuring that both isomers coexist in the ground state.

Finally, although the MS/MS pattern of solution B shows equal intensities of the daughter ions GH$^+$ and CH$^+$, the isomer selected MS/MS obtained from the DIMS-CID experiments indicates that in the case of the Hoo isomer the CH$^+$ fragment is twice more abundant than the GH$^+$ fragment. This is counterintuitive because the proton affinity of N(7)G (960.1 kJ/mol) is larger than the proton affinity of N(3)C (955.5 kJ/mol).[40] However, this anomalous dissociation is in agreement with previous results[41] suggesting that the Cook's kinetics method[42,43] for determining the proton affinity of C and G is not completely applicable to this system.

From the results of this work, three conclusions are highlighted:

(1) The protonated CGH$^+$ WC or Hoo isomers can be prepared in solution and isolated by DIMS, and their structure is preserved upon the ESI process. This can be significant for the experimental study of the structure and PT reactions within the pairs, relevant in point mutations, as suggested earlier by Löwdin.[3]
(2) The DIMS-MS/MS(CID) patterns and IRMPD fingerprints of each isomer allow unequivocal assignment of them. This is expected to be applicable as an easy methodology based on MS/MS and/or IRMPD to determine the existence of Hoo pairs associated with diseases and mutations in real samples.
(3) The detailed dynamics governing the PT should be carefully considered in application of the Cook's kinetic method for determination of the proton affinities of these bases.

EXPERIMENTAL AND COMPUTATIONAL METHODS

Two solutions containing 400 μM C and 400 μM G were prepared in a methanol/water 50:50 solvent. The pH of solution A was 5.8, while in the case of solution B, acetic acid was added to increase the acidity up to pH = 3.2.

In both cases, the CGH$^+$ ion (m/z 263) was mass selected in the quadrupole mass filter stage of a hybrid FT-ICR mass spectrometer (7T FT-ICR Bruker Apex Qe), subsequently accumulated in the hexapole trap, and finally fragmented by CID (at 10^{-3} mbar of Ar and 0.5 V) in the same trap or by

DOI: 10.1021/acs.jpclett.7b02140
J. Phys. Chem. Lett. 2017, 8, 5501−5506

IRMPD in the ICR cell by irradiation with the FEL of CLIO,[35] assisted or not by a CO_2 laser.[36]

By monitoring the intensities of parent (I_{parent}) and resulting fragment ions ($I_{fragment}$) as a function of the laser frequency, the IRMPD spectra were obtained as the fragmentation efficiency $Y = -\ln(I_{parent}/[I_{parent} + \sum I_{fragment}])$.

DIMS has also been used to probe the isomeric diversity of CGH^+. A Bruker Esquire 3000+ instrument has been used, and details can be found elsewhere.[44] The DIMS device is mounted at the place of the spray shield. Ions drift axially between two parallel electrodes transported by a gas flow from atmospheric pressure down to the capillary transfer. Space separation of the ions relies on their radial oscillations induced by an asymmetric radio frequency electric field applied on the two electrodes. A dc offset, called the CV, is applied to one electrode and can be adjusted allowing for the selection of specific ions.[45] In the case of DIMS-MS/MS(CID) experiments, He was used as the collider and the collision voltage was set at 0.2 V.

The potential energy surface of the CGH^+ complex was explored by hybrid density functional calculations at the M06-2X level using the 6-311G++(d, p) basis set for the C, H, N, and O atoms. All of the gas-phase optimizations were performed on a counterpoise-corrected PES because, for relatively flat PESs, this method gives more precise geometrical parameters and therefore more accurate vibrational frequencies (see the SI).[46] The solvent effect was accounted for the D-PCM. All of the calculations were performed with the Gaussian 09 suite of programs.[37]

The relative Gibbs free energies were computed at the same theory level and at 298 K because it has been established that the temperature of the ions (thermalized by collisions with He) in the 3-D quadrupole ion trap[47] used for the DIMS experiments and in the hexapole linear trap of the hybrid FT-ICR (thermalized by collisions with Ar) used for the IRMPD experiments[48] is close to room temperature.

Spectral assignment was achieved by comparing experimental IRMPD spectra and calculated linear IR spectra. The calculated vibrational frequencies were corrected by a factor of 0.983.[38] The IR linear absorption spectra of each minimum of energy were computed at the same level of theory. For the sake of comparison, calculated bands were convoluted assuming a Gaussian profile with a 10 cm^{-1} full width at half-maximum (fwhm), while the IRMPD line width intrinsically depends on the finite laser bandwidth of 0.5% of the central wavelength (corresponding to $\Delta\nu$ = 5.0−10.5 cm^{-1} for ν = 1000−2000 cm^{-1}). It should be noted that, as usual in IRMPD spectroscopy, the relative calculated intensities do not necessarily fit the experimental one due to the linear and nonlinear character of the theoretical and experimental spectra, respectively.

■ ASSOCIATED CONTENT

Supporting Information

The Supporting Information is available free of charge on the ACS Publications website at DOI: 10.1021/acs.jpclett.7b02140.

Isomer calculations, energy and structures of the calculated isomers, comparison of the experimental IRMPD spectrum of solution A with the calculated IR spectra of the most stable isomers likely produced in solution A, potential energy curve along the proton transfer coordinate for the Hoo pair, comparison of relative energies and geometrical parameters calculated with and without a counterpoise-corrected PES, and comparison of the IR spectra calculated with and without a counterpoise-corrected PES (PDF)

■ AUTHOR INFORMATION

Corresponding Authors

*E-mail: gpino@fcq.unc.edu.ar (G.A.P.).
*E-mail: philippe.maitre@u-psud.fr (P.M.).

ORCID

Francis Berthias: 0000-0001-5178-8967
Philippe Maitre: 0000-0003-2924-1054
Gustavo A. Pino: 0000-0002-8702-2688

Present Address

⊥M.B.: Departamento de Física, Facultad de Ciencias Físicas y Matemáticas, Universidad de Chile, Santiago, Chile.

Notes

The authors declare no competing financial interest.

■ ACKNOWLEDGMENTS

This work was conducted under the International Associated Laboratory LIA/LEMIR (CONICET-CNRS). Financial support from FONCyT, CONICET, SeCyT-UNC, European Community's Horizon 2020 Programme (INFRAIA-01-2016, under Grant Agreement No. 730872), and French FT-ICR network (FR3624CNRS) is gratefully acknowledged. P.M. thanks the CNRS and Université Paris-Sud for research funding. The authors also acknowledge all of the suggestions of the referees, in particular, the recommendation of incorporating the double-well potential connecting both Hoo isomers.

■ REFERENCES

(1) Watson, J. D.; Crick, F. H. Molecular Structure of Nucleic Acids: A Structure for Deoxyribose Nucleic Acid. *Nature* **1953**, *171*, 737−738.

(2) Hoogsteen, K. The Crystal and Molecular Structure of a Hydrogen-Bonded Complex Between 1-Methylthymine and 9-Methyladenine. *Acta Crystallogr.* **1963**, *16*, 907−916.

(3) Lowdin, P. O. Proton Tunneling in DNA and its Biological Implications. *Rev. Mod. Phys.* **1963**, *35*, 724−732.

(4) Bertran, J.; Blancafort, L.; Noguera, M.; Sodupe, M. Proton Transfer in DNA Base Pairs. In *Computational Studies of RNA and DNA*; Sponer, J., Lankas, F., Eds.; Springer: The Netherlands, 2006.

(5) de Vries, M. S.; Nir, E.; Kleinermanns, K. Pairing of Isolated Nucleic-Acid Bases in the Absence of the DNA Backbone. *Nature* **2000**, *408*, 949−951.

(6) Feketeová, L.; Chan, B.; Khairallah, G. N.; Steinmetz, V.; Maitre, P.; Radom, L.; O'Hair, R. A. J. Watson−Crick Base Pair Radical Cation as a Model for Oxidative Damage in DNA. *J. Phys. Chem. Lett.* **2017**, *8*, 3159−3165.

(7) Han, S. Y.; Lee, S. H.; Chung, J.; Oh, H. B. Base-Pair Interactions in the Gas-Phase Proton-Bonded Complexes of C^+G and C^+GC. *J. Chem. Phys.* **2007**, *127*, 245102.

(8) Arcella, A.; Portella, G.; Orozco, M. Structure of Nucleic Acids in the Gas Phase. In *Nucleic Acids in the Gas Phase*; Gabelica, V., Ed.; Springer-Verlag: Berlin, Germany, 2014; Chapter 3, 55−76.

(9) Pramanik, S.; Nakamura, K.; Usui, K.; Nakano, S.; Saxena, S.; Matsui, J.; Miyoshi, D.; Sugimoto, N. Thermodynamic Stability of Hoogsteen and Watson−Crick Base Pairs in the Presence of Histone H3-Mimicking Peptide. *Chem. Commun.* **2011**, *47*, 2790−2792.

(10) Tateishi-Karimata, H.; Nakano, M.; Sugimoto, N. Comparable Stability of Hoogsteen and Watson−Crick Base Pairs in Ionic Liquid Choline Dihydrogen Phosphate. *Sci. Rep.* **2015**, *4*, 3593/1−3593/7.

DOI: 10.1021/acs.jpclett.7b02140
J. Phys. Chem. Lett. 2017, 8, 5501−5506

(11) Alvey, H. S.; Gottardo, F. L.; Nikolova, E. N.; Al-Hashimi, H. M. Widespread Transient Hoogsteen Base Pairs in Canonical Duplex DNA with Variable Energetics. *Nat. Commun.* **2014**, *5*, 4786/1−4786/8.
(12) Gacy, A. M.; Goellner, G. M.; Spiro, C.; Chen, X.; Gupta, G.; Bradbury, E. M.; Dyer, R. B.; Mikesell, M. J.; Yao, J. Z.; Johnson, A. J.; Richter, A.; Melancon, S. B.; McMurray, C. T. GAA Instability in Friedreich's Ataxia Shares a Common, DNA-Directed and Intraallelic Mechanism with Other Trinucleotide Diseases. *Mol. Cell* **1998**, *1*, 583−593.
(13) Mirkin, S. M. Expandable DNA Repeats and Human Disease. *Nature* **2007**, *447*, 932−940.
(14) Vasquez, K. M.; Narayanan, L.; Glazer, P. M. Specific Mutations Induced by Triplex-Forming Oligonucleotides in Mice. *Science* **2000**, *290*, 530−533.
(15) Nikolova, E. N.; Kim, E.; Wise, A. A.; O'Brien, P. J.; Andricioaei, I.; Al-Hashimi, H. Transient Hoogsteen Base Pairs in Canonical Duplex DNA. *Nature* **2011**, *470*, 498−502.
(16) Honig, B.; Rohs, R. Flipping Watson and Crick. *Nature* **2011**, *470*, 472−473.
(17) Nair, D. T.; Johnson, R. E.; Prakash, S.; Prakash, L.; Aggarwal, A. K. Replication by Human DNA Polymerase-Iota Occurs by Hoogsteen Base-Pairing. *Nature* **2004**, *430*, 377−380.
(18) Lin, Y.; Wang, H.; Gao, S.; Schaefer, H. F., III Hydrogen-Bonded Proton Transfer in the Protonated Guanine-Cytosine (GC+H)$^+$ Base Pair. *J. Phys. Chem. B* **2011**, *115*, 11746−11756.
(19) Bende, A.; Muntean, C. M. The Influence of Anharmonic and Solvent Effects on the Theoretical Vibrational Spectra of the Guanine-Cytosine Base Pairs in Watson-Crick and Hoogsteen Configurations. *J. Mol. Model.* **2014**, *20*, 2113/1−2113/12.
(20) *Nucleic Acids in the Gas Phase*; Gabelica, V., Ed.; Springer-Verlag: Berlin, Germany, 2014.
(21) Berdakin, M.; Féraud, G.; Dedonder-Lardeux, C.; Jouvet, C.; Pino, G. A. Effect of Ag^+ on the Excited-State Properties of a Gas-Phase $(Cytosine)_2Ag^+$ Complex: Electronic Transition and Estimated Lifetime. *J. Phys. Chem. Lett.* **2014**, *5*, 2295−2301.
(22) Gao, J.; Berden, G.; Rodgers, M. T.; Oomens, J. Interaction of Cu^+ with Cytosine and Formation of i-Motif-Like C−M^+−C Complexes: Alkali versus Coinage Metals. *Phys. Chem. Chem. Phys.* **2016**, *18*, 7269−7277.
(23) Rodgers, M. T.; Armentrout, P. B. Cationic Noncovalent Interactions: Energetics and Periodic Trends. *Chem. Rev.* **2016**, *116*, 5642−5687.
(24) Taccone, M.; Féraud, G.; Berdakin, M.; Dedonder-Lardeux, C.; Jouvet, C.; Pino, G. A. Communication: UV Photoionization of Cytosine Catalyzed by Ag^+. *J. Chem. Phys.* **2015**, *143*, 041103.
(25) Nosenko, Y.; Menges, F.; Riehn, C.; Niedner-Schatteburg, G. Investigation by Two-Color IR Dissociation Spectroscopy of Hoogsteen-type Binding in a Metalated Nucleobase Pair Mimic. *Phys. Chem. Chem. Phys.* **2013**, *15*, 8171−8178.
(26) Power, B.; Haldys, V.; Salpin, J. Y.; Fridgen, T. D. Structures of $[M(Ura\text{-}H)(Ura)]^+$ and $[M(Ura\text{-}H)(H_2O)_n]^+$ (M = Cu, Zn, Pb; n = 1−3) Complexes in the Gas Phase by IRMPD Spectroscopy in the Fingerprint Region and Theoretical Studies. *Int. J. Mass Spectrom.* **2017**, DOI: 10.1016/j.ijms.2017.05.003.
(27) Berdakin, M.; Féraud, G.; Dedonder-Lardeux, C.; Jouvet, C.; Pino, G. A. Excited States of Protonated DNA/RNA Bases. *Phys. Chem. Chem. Phys.* **2014**, *16*, 10643−10650.
(28) Pedersen, S. Ø.; Støchkel, K.; Byskov, C. S.; Baggesen, L. M.; Nielsen, S. B. Gas-Phase Spectroscopy of Protonated Adenine, Adenosine 5′-Monophosphate and Monohydrated Ions. *Phys. Chem. Chem. Phys.* **2013**, *15*, 19748−19752.
(29) Salpin, J. Y.; Guillaumont, S.; Tortajada, J.; MacAleese, L.; Lemaire, J.; Maitre, P. Infrared Spectra of Protonated Uracil, Thymine and Cytosine. *ChemPhysChem* **2007**, *8*, 2235−2244.
(30) Wu, R. R.; He, C. C.; Hamlow, L. A.; Nei, Y. − W.; Berden, G.; Oomens, J.; Rodgers, M. T. N3 Protonation Induces Base Rotation of 2′-Deoxyadenosine-5′-Monophosphate and Adenosine-5′-Monophosphate. *J. Phys. Chem. B* **2016**, *120*, 4616−4624.
(31) Féraud, G.; Berdakin, M.; Dedonder-Lardeux, C.; Jouvet, C.; Pino, G. A. Excited States of Proton-Bound DNA/RNA Base Homodimers: Pyrimidines. *J. Phys. Chem. B* **2015**, *119*, 2219−2228.
(32) Yang, B.; Rodgers, M. T. Base-Pairing Energies of Proton-Bound Heterodimers of Cytosine and Modified Cytosines: Implications for the Stability of DNA i-Motif Conformations. *J. Am. Chem. Soc.* **2014**, *136*, 282−290.
(33) Lapthorn, C.; Pullen, F.; Chowdhry, B. Z. Ion Mobility Spectrometry-Mass Spectrometry (IMS-MS) of Small Molecules: Separating and Assigning Structures to Ions. *Mass Spectrom. Rev.* **2013**, *32*, 43−71.
(34) Hoaglund-Hyzer, C. S.; Li, J.; Clemmer, D. E. Mobility Labeling for Parallel CID of Ion Mixtures. *Anal. Chem.* **2000**, *72*, 2737−2740.
(35) Bakker, J. M.; Besson, T.; Lemaire, J.; Scuderi, D.; Maitre, P. Gas-Phase Structure of a π-Allyl−Palladium Complex: Efficient Infrared Spectroscopy in a 7 T Fourier Transform Mass Spectrometer. *J. Phys. Chem. A* **2007**, *111*, 13415−13424.
(36) Sinha, R. K.; Nicol, E.; Steinmetz, V.; Maitre, P. Gas Phase Structure of Micro-Hydrated $[Mn(ClO_4)]^+$ and $[Mn_2(ClO_4)_3]^+$ Ions Probed by Infrared Spectroscopy. *J. Am. Soc. Mass Spectrom.* **2010**, *21*, 758−772.
(37) Frisch, M. J.; Trucks, G. W.; Schlegel, H. B.; Scuseria, G. E.; Robb, M. A.; Cheeseman, J. R.; Scalmani, G.; Barone, V.; Mennucci, B.; Petersson, G. A.;*Gaussian 09*, revision D.01; Gaussian Inc.: Wallingford, CT, 2009.
(38) Alecu, I. M.; Zheng, I.; Zhao, Y.; Truhlar, D. G. Computational Thermochemistry: Scale Factor Databases and Scale Factors for Vibrational Frequencies Obtained from Electronic Model Chemistries. *J. Chem. Theory Comput.* **2010**, *6*, 2872−2887.
(39) Verdolino, V.; Cammi, R.; Munk, B. H.; Schlegel, H. B. Calculation of p*Ka* Values of Nucleobases and the Guanine Oxidation Products Guanidinohydantoin and Spiroiminodihydantoin using Density Functional Theory and a Polarizable Continuum Model. *J. Phys. Chem. B* **2008**, *112*, 16860−16873.
(40) Nguyen, M. T.; Uchimaru, T.; Zeegers-Huyskens, T. Protonation and Deprotonation Enthalpies of Guanine and Adenine and Implications for the Structure and Energy of Their Complexes with Water: Comparison with Uracil, Thymine, and Cytosine. *J. Phys. Chem. A* **1999**, *103*, 8853−8860.
(41) Seong, Y.; Han, S. Y.; Jo, S.; Oh, H. B. An Anomalous Dissociation of Protonated Cluster Ions of DNA Guanine-Cytosine Base-Pair. *Mass Spectrom. Lett.* **2011**, *2*, 73−75.
(42) Cooks, R. G.; Koskinen, J. T.; Thomas, P. D. The Kinetic Method of Making Thermochemical Determinations. *J. Mass Spectrom.* **1999**, *34*, 85−92.
(43) Di Donna, L.; Napoli, A.; Sindona, G.; Athanassopoulos, C. A Comprehensive Evaluation of the Kinetic Method Applied in the Determination of the Proton Affinity of the Nucleic Acid Molecules. *J. Am. Soc. Mass Spectrom.* **2004**, *15*, 1080−1086.
(44) Hernández, O.; Isenberg, S.; Steinmetz, V.; Glish, G. L.; Maitre, P. Probing Mobility-Selected Saccharide Isomers: Selective Ion−Molecule Reactions and Wavelength-Specific IR Activation. *J. Phys. Chem. A* **2015**, *119*, 6057−6064.
(45) Schneider, B. B.; Nazarov, E. G.; Londry, F.; Vouros, P.; Covey, T. R. Differential Mobility Spectrometry/Mass Spectrometry History, Theory, Design Optimization, Simulations, and Applications. *Mass Spectrom. Rev.* **2016**, *35*, 687−737.
(46) Plumley, J. A.; Dannenberg, J. J. A Comparison of the Behavior of Functional/Basis Set Combinations for Hydrogen-Bonding in the Water Dimer with Emphasis on Basis Set Superposition Error. *J. Comput. Chem.* **2011**, *32*, 1519−1527.
(47) Gronert, S. Estimation of Effective Ion Temperatures in a Quadrupole Ion Trap. *J. Am. Soc. Mass Spectrom.* **1998**, *9*, 845−848.
(48) Hernández, O.; Paizs, B.; Maitre, P. Rearrangement Chemistry of a_n Ions Probed by IR Spectroscopy. *Int. J. Mass Spectrom.* **2015**, *377*, 172−178.

DOI: 10.1021/acs.jpclett.7b02140
J. Phys. Chem. Lett. 2017, 8, 5501−5506